Behavioral/Systems/Cognitive

Distribution and Injury-Induced Plasticity of Cadherins in Relationship to Identified Synaptic Circuitry in Adult Rat Spinal Cord

John H. Brock, Alice Elste, and George W. Huntley
Fishberg Department of Neuroscience, The Mount Sinai School of Medicine, New York, New York 10029

Cadherins are synaptically enriched cell adhesion and signaling molecules. In brain, they function in axon targeting and synaptic plasticity. In adult spinal cord, their localization, synaptic affiliation, and role in injury-related plasticity are mostly unexplored. Here, we demonstrate in adult rat dorsal horn that E- and N-cadherin display unique patterns of localization to functionally distinct types of synapses of intrinsic and primary afferent origin. Within the nociceptive afferent pathway to lamina II, nonpeptidergic C-fiber synapses in the deeper half of lamina II (IIi) contain E-cadherin but mostly lack N-cadherin, whereas the majority of the peptidergic C-fiber synapses in the outer half of lamina II (IIo) contain N-cadherin but lack E-cadherin. Approximately one-half of the Aβ-fiber terminations in lamina III contain N-cadherin; none contain E-cadherin. Strikingly, the distribution and levels of these cadherins are differentially affected by sciatic nerve axotomy, a model of neuropathic pain in which degenerative and regenerative structural plasticity has been implicated. Within the first 7 d after axotomy, E-cadherin is rapidly and completely lost from the dorsal horn synapses with which it is affiliated, whereas N-cadherin localization and levels are unchanged; such patterns persist through 28 d postlesion. The loss of E-cadherin thus occurs before the onset of mechanical hyperalgesia (~10–21 d postlesion), as reported previously. Together, the synaptic specificity displayed by these cadherins, coupled with their differential response to injury, suggests that they may proactively contribute to the maintenance of some, and incipient dismantling of other, synaptic circuits in response to nerve injury. Speculatively, such changes may ultimately contribute to subsequently emerging abnormalities in pain perception.

Key words: **substantia gelatinosa; C-fibers; Aβ-fibers; cell adhesion molecules; sciatic nerve lesion; neuropathic pain**

Introduction

Sensory stimuli from the surface and deeper tissues of the body are relayed to higher CNS centers through synapses formed between the central terminations of primary afferent axons and neurons of the spinal dorsal horn. Such terminations of nociceptive, thermoreceptive, and mechanoreceptive afferents are distributed with precise order across dorsal horn layers and together represent a variety of functionally, structurally, and neurochemically distinct synaptic circuits through which somatosensory stimuli are perceived (Szentágothai, 1964; Cervero and Iggo, 1980; Ruda et al., 1986).

Peripheral nerve injury leads to aberrant sensory perception, particularly neuropathic pain syndromes. The circuitry involved includes dorsal horn lamina I and II terminations of nociceptive unmyelinated C-fibers and thinly myelinated A∂-fibers (Mantyh et al., 1997; Vulchanova et al., 2001; Khasabov et al., 2002) and reflects, in part, changes in neurochemistry of these circuits (Woolf and Salter, 2000). In addition, peripheral nerve crush or axotomy is associated with synaptic structural plasticity within the neuropil of lamina II. Such plasticity includes synaptic and terminal degeneration of certain C-fiber nociceptive afferents (Knyihar and Csillik, 1976; Kapadia and LaMotte, 1987), as well as sprouting and regeneration of synaptic contacts in which remaining C-fibers or mechanoreceptive Aβ-fibers have been implicated (Csillik and Knyihar, 1975; Woolf et al., 1992; Koerber et al., 1994; Kohama et al., 2000). The molecular mechanisms that specify dorsal horn synaptic circuitry and contribute to injury-related structural synaptic plasticity and retargeting are mostly unexplored. Such knowledge bears generally on strategies for promoting appropriate retargeting of spinal circuits damaged or lost by injury (Horner and Gage, 2000), in which successful recovery of function may depend critically on molecular recognition codes that ensure correct presynaptic to postsynaptic matching of central synaptic connections.

Classic cadherins are a family of synaptically enriched transmembrane glycoproteins mediating Ca^{2+}-dependent homophilic adhesion (Geiger and Ayalon, 1992). They are differentially associated with functionally distinct synapses and play critical roles in laminar targeting of axon terminations in thalamocortical pathways (Huntley and Benson, 1999; Gil et al., 2002; Poskanzer et al., 2003) and in other systems (Inoue and

Received July 8, 2004; revised Aug. 26, 2004; accepted Aug. 30, 2004.

This work was supported by Predoctoral Fellowship NS44718-01 and Grant NS044068 from the National Institutes of Health (National Institute of Neurological Disorders and Stroke) and Grant HB1-0104-2 from the Christopher Reeve Paralysis Foundation. We are grateful to Dr. Deanna Benson for helpful comments.

Correspondence should be addressed to Dr. George W. Huntley, Fishberg Department of Neuroscience, The Mount Sinai School of Medicine, Box 1065, 1425 Madison Avenue, New York, NY 10029. E-mail: george.huntley@mssm.edu.

DOI:10.1523/JNEUROSCI.2726-04.2004

 0270-6474/04/248806-12$15.00/0

Sanes, 1997). Cadherins also participate actively in synaptic structural and functional plasticity. In the hippocampus, N-cadherin is upregulated in dentate gyrus granule cells as mossy fibers sprout during epileptogenesis (Shan et al., 2002) and contributes to synaptic plasticity of area CA1 during hippocampal long-term potentiation (Tang et al., 1998; Bozdagi et al., 2000). In spinal cord, cadherins and protocadherins play developmental roles in early spinal cord differentiation (Fredette and Ranscht, 1994; Marthiens et al., 2002; Price et al., 2002; Wang et al., 2002). However, their organization and synaptic affiliation with identified circuitry in adulthood has not been examined.

Here, we examine in detail the synaptic affiliation and nerve injury response of two classic cadherins: E-cadherin, because it is associated with small-diameter dorsal root ganglion (DRG) neurons with unmyelinated axons (Shimamura et al., 1992; Uchiyama et al., 1994; Seto et al., 1997), and N-cadherin, because of its well documented role in synaptic circuit development and plasticity (Huntley, 2002).

Materials and Methods

Animal use and sciatic nerve axotomy. All animals were maintained and treated in strict accordance with protocols approved by the Institutional Animal Care and Use Committee of Mount Sinai as well as with guidelines advocated by the National Institutes of Health. A total of 99 adult male Sprague Dawley rats (>60 d old) were used in these studies. Fifteen animals were killed by intracardiac perfusion, and their lumbar spinal cords were subjected to immunolabeling. Eighty-four animals were deeply anesthetized with a mixture of ketamine (40 mg/kg) and xylazine (10 mg/kg). The sciatic nerve was exposed bilaterally at midthigh level. In 44 of these animals, the right sciatic nerve was transected with iris scissors, and an ~1 mm segment was removed to prevent peripheral regeneration. Five of these animals received, at 4 d after axotomy, an injection of 1 μl of 4% wheat germ agglutinin conjugated to horseradish peroxidase (WGA–HRP) (Vector Laboratories, Burlingame, CA) into the sciatic nerve proximal to the cut. These animals were allowed to survive an additional 3 d for transport. In all animals, the left side served as a sham-operated control in which the nerve was exposed but not transected. In the other 40 animals, sciatic nerves were injected with transganglionic tracers described below. In all cases, overlying muscles, fascia, and skin were sutured in layers, and the animals were allowed to recover for variable periods ranging from 1 to 28 d. Animals were administered buprenorphine (0.05 mg/kg, i.m.) daily until sacrifice.

Injection of transganglionic tracers and perfusion. Injections of various tracers were placed directly into the exposed sciatic nerves using a Hamilton syringe. Each nerve received only a single tracer. In 10 animals, 2 μl of 2% cholera toxin-B (CTB)–Alexa 488 (Molecular Probes, Eugene, OR) dissolved in distilled H_2O was injected; animals survived 3 d to allow for transport. Animals were deeply anesthetized with a mixture of ketamine and xylazine, as described above, and perfused through the left ventricle first with 100 ml of cold 1% paraformaldehyde (in 0.1 M PBS, pH 7.4), followed by 10 min of cold 4% paraformaldehyde in PBS. In 30 animals, 1 μl of 1.5% CTB–HRP (Sigma, St. Louis, MO) or 1 μl of 4% WGA–HRP (Vector Laboratories) were injected. After a survival period of 3 d, animals were deeply anesthetized and perfused with a mixture of aldehydes (2% paraformaldehyde and 2% glutaraldehyde). This material was used for light and electron microscopy described below.

Primary antibodies and isolectin B4. The following primary antibodies were used for light microscopy: mouse anti-E-cadherin (1:200; BD Biosciences, San Jose, CA), mouse anti-N-cadherin (1:400; BD Biosciences), rabbit anti-glutamic acid decarboxylase (GAD)-65 (1:1000; Chemicon, Temecula, CA), rabbit anti-neurotensin (NT; 1:1000; Bachem, King of Prussia, PA), rabbit anti-somatostatin (1:1000; Bachem), rat anti-substance P (1:100; Chemicon), guinea pig anti-calcitonin gene-related peptide (CGRP; 1:500; Bachem), vesicular glutamate transporters 1 and 2 (vGluts; 1:20,000 and 1:1000, respectively; Chemicon), and rabbit anti-synaptophysin (1:200; Zymed, San Franscisco, CA). Isolectin B4 (IB4)–biotin (1:1000) was obtained from Sigma. For immunoelectron microscopy, we used mouse anti-E- and anti-N-cadherin antibodies from BD Biosciences (both at 25 μg/ml) or rabbit anti-N-cadherin antibody (3.5 μg/ml; gift from Dr. David Colman, Montreal Neurological Institute, Montreal, Quebec, Canada) (Tanaka et al., 2000).

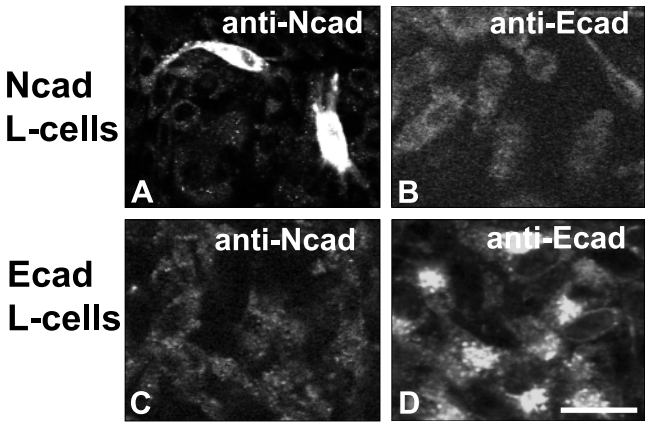

Figure 1. Specificity of N-cadherin and E-cadherin antibodies. L-cells expressing N-cadherin (*A*, *B*) or E-cadherin (*C*, *D*) were incubated with mouse anti-N-cadherin (*A*, *C*) or anti-E-cadherin (*B*, *D*) antibodies. The anti-N-cadherin antibody labels N-cadherin L-cells (*A*) but does not label E-cadherin-expressing L-cells (*C*); conversely, the anti-E-cadherin antibody labels E-cadherin L-cells (*D*) but does not label N-cadherin-expressing L-cells (*B*). Scale bar, 10 μm.

Immunofluorescence. The L4/L5 lumbar segment was removed, post-fixed for 6 hr at 4°C in the same fixative, then cryoprotected in 30% sucrose at 4°C for 2 d. Fifty-micrometer-thick sections were cut on a freezing microtome and placed into blocking solution consisting of 3% bovine serum albumin (BSA) plus 5% normal serum in 0.01 M phosphate buffer (PB) for 1 hr at room temperature. For single labeling, sections were then incubated in primary antibodies overnight at 4°C in diluent consisting of 0.5% BSA plus 1% normal serum. Sections were then incubated in species-appropriate secondary antibodies directly conjugated to Alexa 488 (1:400; Molecular Probes). For visualizing IB4 binding, BSA was omitted from all steps; sections were incubated in IB4–biotin overnight in PB, followed by incubation in streptavidin–Alexa 488 (1:400; Molecular Probes). For double and triple labeling, sections were incubated in two or three species-distinct primary antibodies simultaneously, followed by incubation with species-appropriate combinations of secondary antibody conjugates Alexa 488, Alexa 568, and Alexa 594 (1:400 each; Molecular Probes) and streptavidin–cyanine 5 (1:100; Jackson ImmunoResearch, West Grove, PA), all for 1 hr at room temperature. Sections were mounted on gelatin-subbed slides and coverslipped with Vectashield (Vector Laboratories). To control for nonspecific reactivity of the secondary antibodies, tissue sections were processed as described, except for omitting the primary antibody. No label was seen when primary antibody was omitted. Specificity of the mouse anti-cadherin antibodies was verified using cadherin-transfected L-cells as described below and shown in Figure 1.

L-cell immunocytochemistry and specificity of cadherin primary antibodies. L-cells stably expressing E-cadherin were a gift from Dr. D. Colman. N-cadherin-expressing L-cells were created by transient transfection with full-length N-cadherin (gift from Dr. Deanna Benson, Mount Sinai, New York, NY) using Lipofectamine-Plus reagent (Invitrogen, Carlsbad, CA) according to the manufacturer's instructions. Confluent cells were fixed in 4% paraformaldehyde, permeabilized with 0.25% Triton X-100, and processed immunofluorescently for mouse E-cadherin and mouse N-cadherin antibody binding as described above. As expected, N-cadherin L-cells were labeled with the N-cadherin antibody (Fig. 1*A*), whereas E-cadherin L-cells were labeled by the E-cadherin antibody (Fig. 1*D*). Importantly, no cross-reactivity was observed: E-cadherin antibody did not label N-cadherin L-cells (Fig. 1*B*), nor did the N-cadherin antibody label E-cadherin L-cells (Fig. 1*C*).

Confocal microscope analysis and quantification of synaptic codistribution. Single optical sections through the lumbar dorsal horn were obtained with a Zeiss 410 laser scanning microscope (Zeiss, Thornwood,

Table 1. Quantitative evaluation of cadherin association with identified synaptic circuitry

Source or type of synapse[a]	Marker	Percentage E-cadherin labeled[b]	Percentage N-cadherin labeled[b]	Lamina examined
Primary afferents (unmyelinated)				
Nonpeptidergic C-fibers	IB4	80.4 (90/112)	9.2 (11/120)	IIi
Peptidergic C-fibers	CGRP	N/A	64.5 (80/124)	IIo
Primary afferents (myelinated)				
Aβ-fibers	CTB	N/A	51.4 (57/111)	III
Intrinsic circuitry				
Excitatory intrinsic neurons	NT	29.5 (59/200)	52.6 (60/114)	IIi
Inhibitory intrinsic neurons	GAD	30.2 (32/106)	33.6 (39/116)	IIi

[a]Synaptic puncta were defined as those that immunolabeled for synaptophysin (IB4 or CGRP) or vGluts (CTB or NT) or GAD.

[b]The left-most number is a percentage; values in parentheses are the number of cadherin-labeled synaptic puncta/total number of synaptic puncta. N/A, Not applicable.

NY) equipped with a 100×, 1.4 numerical aperture oil-immersion objective, an argon/krypton laser, a dichroic beam splitter, and filters of 515–540, 575–640, and 670–810 nm. The clear separation of emission spectra was verified by comparing images obtained from two channels simultaneously using the dichroic beam splitter with those obtained sequentially using one laser line. Brightness and contrast settings for labels were kept within close range of each other. To determine the percentage of peptide-, lectin-, or tracer-labeled synaptic puncta that were cadherin positive, a triple-labeling strategy was used. For this analysis, "synaptic puncta" were defined as any peptide-, lectin-, or tracer-labeled punctum that codistributed with labeling for the presynaptic terminal markers vGluts, synaptophysin, or GAD. This criterion was necessary because many of the peptide markers and tracers used for identifying spinal circuitry are not localized exclusively to synaptic regions but are also found in nonsynaptic portions of axons and dendrites. We used labeling for vGluts as the synaptic marker when examining cadherin association with labeling for NT, which labels a population of intrinsic excitatory terminals (Todd and Spike, 1993) or for Aβ-fiber synaptic terminals in lamina III (Li et al., 2003; Todd et al., 2003). We used synaptophysin as the synaptic marker when examining cadherin association with lamina II primary afferent (C-fiber) synapses because vGluts are not present at many of these (Todd et al., 2003). We used GAD as a marker of intrinsic inhibitory synaptic terminals (Ribak et al., 1978). For each peptide marker or primary afferent tracer under investigation, six sections through the L4/L5 lumbar segment were used to acquire 40–50 separate confocal images from each lamina (I–III) of the dorsal horn, collectively tiling a significant portion of the sciatic nerve termination territory (Shortland et al., 1989). Mindful of unequal antibody penetration, optical sections were acquired only at tissue depths in which all three labels were clearly evident. From these images, 100–200 double-labeled puncta (peptide or tracer plus vGluts, synaptophysin, or GAD) were counted, and of these synaptic puncta, the percentage of those that codistributed for cadherin labeling was determined and reported in Table 1. To compare E-cadherin and N-cadherin immunofluorescence after sciatic nerve axotomy, brightness and contrast settings were optimized for cadherin labeling on the contralateral sham-operated side and were not varied when imaging cadherin labeling on the axotomized side. A 16× objective and confocal microscopy was used to image the entire extent of the sciatic nerve termination zone within the L4/L5 dorsal horn.

HRP histochemistry and immunoelectron microscopy. L4/L5 cord segments were postfixed for 4 hr, washed with 0.1 M PB, and sectioned at 50 μm on a vibratome. Sections were reacted for tetramethylbenzidine (TMB) histochemistry following the procedures of Weinberg and van Eyck (1991). Briefly, sections were preincubated in 0.2% TMB with 1% ammonium paratungstate in 0.1 M PB, pH 6.0, for 30 min. The reaction was initiated by the addition of 0.3% H_2O_2 and allowed to proceed until reaction product appeared, usually ~10–20 min. After washes in 0.1 M PB, pH 6.0, sections were mounted on gelatin-subbed slides, dehydrated, and coverslipped. Animals used for electron microscopic analysis were processed as above for HRP histochemistry, except that 350-μm-thick vibratome slices were used. Additionally, the TMB reaction product was further stabilized by incubating sections in 2.5% diaminobenzidine, 1% $CoCl_2$, and 0.3% H_2O_2 for 10 min. After washes in PB, pH 6.0, slices were cryoprotected by immersion in 0.1 M PB, pH 6.0, containing increasing concentrations of glycerol (10–30%). Quadrants of tissue from the dorsal horn were then dissected from the slices and processed by freeze substitution and low-temperature embedding (van Lookeren Campagne et al., 1991; Hjelle et al., 1994; Chaudhry et al., 1995). Sections were plunged rapidly into liquid propane cooled by liquid nitrogen (−190°C) in a Universal Cryofixation System KF80 (Reichert-Jung, Vienna, Austria). The samples were immersed in 1.5% uranyl acetate (for *en bloc* fixation) dissolved in anhydrous methanol (−90°C; 24 hr) in a cryosubstitution AFS unit (Leica, Bannockburn, IL). The temperature was gradually raised in steps of 4°C/hr from −90 to −45°C. The samples were then washed three times with anhydrous methanol and infiltrated with Lowicryl HM20 resin (Electron Micoscopy Sciences, Hatfield, PA) at −45°C with a progressive increase in the ratio of resin to methanol, followed with pure Lowicryl overnight. Blocks were polymerized with UV light (360 nm) at −45°C for 48 hr, followed by 24 hr at room temperature. Ultrathin sections were cut with a diamond knife on a Reichert-Jung ultramicrotome and mounted on nickel grids coated with a film of 0.3% Formvar. For immunolabeling, grids were blocked in Tris-buffered saline (TBS) containing 0.05% Triton X-100 and 2% BSA, then incubated with N-cadherin (mouse or rabbit) or E-cadherin antibodies diluted in the same diluent overnight (for antibody concentrations, see above). Antibody binding was visualized by incubation for 2 hr in species-appropriate secondary antibodies conjugated to 10 nm gold (1:100; Electron Microscopy Sciences). Sections were rinsed, dried, and counterstained with uranyl acetate and lead citrate. Sections were viewed on a Jeol 1200EX electron microscope, and digital images were taken with an Advantage CCD camera (Advanced Microscopy Techniques, Danvers, MA). Control experiments were processed as above, except for replacing primary antibody with mouse isotype-appropriate IgGs or normal rabbit IgG (used at same protein concentrations as corresponding primary antibody; Vector Laboratories). Under these conditions, only occasional gold particles were seen, and none appeared concentrated at junctions. To control for nonspecific reactivity of the gold-conjugated secondary antibodies, grids were processed as described, except for the omission of the primary cadherin antibody. No gold particles were observed under these conditions.

Western blotting and quantification. Cadherin protein levels after sciatic nerve axotomy (see above for details) were determined at various time points by Western blotting. Animals were killed at 4 d ($n = 5$) or 7 d ($n = 7$) after axotomy by CO_2 asphyxiation, and the L4/L5 cord segment was removed rapidly. A 0.75 mm tissue punch was taken through medial lamina I/II, which was visualized with the aid of a dissecting microscope. The tissue was then immediately frozen on dry ice. Tissue was homogenized in SDS sample buffer (100 mM Tris, pH 7.6, 150 mM NaCl, 200 mM sucrose, and 2% SDS) and sonicated for 3 sec. Protein concentration was determined by BCA assay (Pierce, Rockford, IL) in triplicate. Identical samples were then prepared and run on three independent gels. For each sample, 25 μm of total protein were run through a 10% SDS–Tris–HCl gel and transferred to PDVF membrane with a semi-dry transfer apparatus (Bio-Rad, Hercules, CA). Nonspecific antibody binding to membranes was blocked by exposure to 5% milk dissolved in TBS containing 0.05% Tween 20 overnight at 4°C, followed by incubation of membrane with mouse anti-E-cadherin or anti-N-cadherin antibody (1:5000) and rabbit anti-glyceraldehyde phosphate dehydrogenase antibody (GAPDH; 1:5000, Trevigen, Gaithersburg, MD) for 1 hr at room temperature in 2% milk. Membranes were then washed in TBS–Tween 20 and

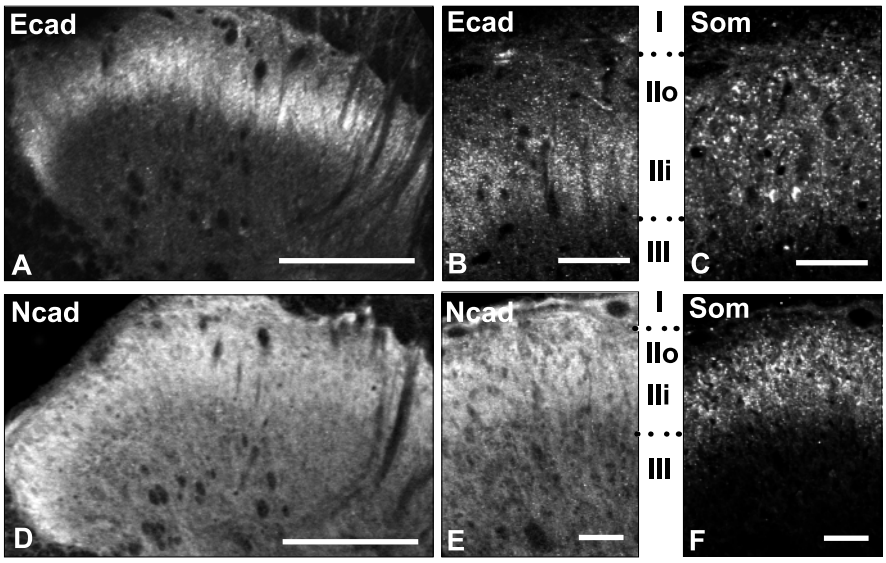

Figure 2. Differential laminar distribution patterns of E- and N-cadherin immunolabeling in dorsal horn. E-cadherin labeling is confined to a dense, superficial band (*A*) corresponding to lamina IIi (*B*), determined by comparison with the lamina II marker somatostatin (Som; *C*, *F*). N-cadherin immunolabeling is broader (*D*) and is more homogeneously distributed throughout all dorsal horn laminas (*E*). In this and subsequent figures, Roman numerals correspond to dorsal horn lamina. IIo, Lamina II outer; IIi, lamina II inner. In all images, medial is to the right. Scale bars: *A*, *D*, 100 μm; *B*, *C*, *E*, *F*, 50 μm.

incubated in sheep anti-mouse-HRP and donkey anti-rabbit-HRP (both 1:2500; Amersham Biosciences, Piscataway, NJ) in 2% milk for 1 hr at room temperature. Membranes were developed in the ECL system (Pierce) for 1 min and exposed to Kodak X-OMAT autoradiography film (Sigma). Film autoradiograms were scanned using identical parameters into Adobe Photoshop 7.0 (Adobe Systems, Mountain View, CA). To compare N-cadherin protein levels across post-axotomy days, band intensities for N-cadherin and GAPDH were determined using MetaMorph software (Universal Imaging, Downingtown, PA). To adjust for differences in background across lanes, lane intensity was determined from a sampling region identical to that used to measure the specific bands and subtracted from the intensities of the corresponding N-cadherin and GAPDH bands. For each lane, N-cadherin band intensity was normalized to GAPDH band intensity within the same lane. Ratios of N-cadherin band intensity to GAPDH band intensity (OD Ncad/OD gapdh) were determined for sham-operated, 4 and 7 d post-axotomy time points, and the means of ratios (+SEM) were plotted. Two-tailed *t*-tests were used to determine significant differences in ratios. A p value <0.05 was considered significant. No significant differences were seen between the 4 d sham and the 7 d sham, thus these values were combined.

Figure preparation. Digital images were imported into Adobe Photoshop 7.0 where minimal adjustments in contrast and brightness were made. Multi-panel figure layout and graphics were completed using QuarkXpress 4.1 (Quark, Denver, CO).

Results

Laminar distribution of E- and N-cadherin in lumbar dorsal horn

We first investigated the overall laminar distributions of E- and N-cadherin in the adult lumbar dorsal horn by using cadherin type-specific antibodies (Fig. 1) to immunolabel tissue sections from adult rat spinal cord (Fig. 2). E- and N-cadherin are both present in dorsal horn gray matter but display distinct laminar distribution patterns. E-cadherin immunoreactivity is restricted to a dense, superficially located band that extends evenly across the mediolateral extent of the dorsal horn (Fig. 2*A*). Comparison with immunolabeling for somatostatin, a marker of laminas I–II (Todd and Spike, 1993), reveals that E-cadherin is localized to the ventral half of lamina II (IIi), with only very sparse label in the dorsal half (IIo) (Fig. 2*B*,*C*). Outside of lamina II, E-cadherin immunolabel is absent. N-cadherin labeling also extends evenly across the mediolateral extent of the dorsal horn but is more broadly distributed than E-cadherin in the dorsoventral axis (Fig. 2*D*). Comparison with the laminar somatostatin labeling pattern reveals that N-cadherin is densely and homogeneously distributed throughout laminas I–II, with no sublaminar distinctions apparent as they are with E-cadherin (Fig. 2*E*,*F*). Additionally, N-cadherin immunolabel extends more deeply throughout the dorsal horn to include lamina III–V (Fig. 2*D*,*E*).

E- and N-cadherin localize to synapses in lumbar dorsal horn

Inspection of higher-magnification images reveals that E- and N-cadherin immunolabel is punctate. We next investigated whether such puncta correspond to synapses, as they mostly do in brain (Yamagata et al., 1995; Fannon and Colman, 1996; Uchida et al., 1996; Arndt et al., 1998; Benson and Tanaka, 1998; Huntley and Benson, 1999; Bozdagi et al., 2000). We first used confocal microscopy to analyze tissue sections immunofluorescently labeled for E- or N-cadherin and for the vGluts. vGluts, when used together, localize to a majority of excitatory synaptic terminals within the spinal gray matter (Li et al., 2003; Todd et al., 2003). This was followed by immunogold electron microscopy to verify the light microscopic localization patterns.

Many, but not all, E-cadherin puncta codistribute with puncta labeled for vGluts (Fig. 3*A*-*C*). In general, E-cadherin puncta that codistribute with vGluts appear larger in comparison with smaller ones that rarely show codistribution. As in brain, the codistribution pattern is characterized by partial overlap of the cadherin and vGlut labels, producing a central region of codistribution (Fig. 3*C*, yellow pixels and arrows). The localization of E-cadherin to asymmetric synaptic junctions within lamina IIi was verified by immunogold electron microscopy (Fig. 3*D*,*E*).

Similar to E-cadherin, both large and small N-cadherin puncta are found throughout the dorsal horn neuropil. Many of these, but not all, codistribute with puncta labeled for vGluts throughout laminas I–V (Fig. 4*A*–*C*). Those that show codistribution also appear to be the larger ones. We verified localization of N-cadherin to the synaptic junctional complex in lamina IIo by immunogold electron microscopy (Fig. 4*D*,*E*). In contrast to E-cadherin localization, N-cadherin gold particles are found at symmetrically thick membrane densities characteristic of puncta adherens (Fig. 4*D*, arrowhead). Such N-cadherin-labeled puncta adherens are immediately adjacent to conventional asymmetric synaptic junctions that lack N-cadherin gold particles (Fig. 4*D*, arrow), collectively forming the synaptic junctional complex (Peters et al., 1991). In addition to labeling of puncta adherens, gold particles are also found at some axo-axonic synaptic junctions (Fig. 4*E*, arrowhead), a well recognized component of spinal lamina II circuitry (Ribeiro-da-Silva and Coimbra, 1982). In lamina III, gold particles are found at conventional asymmetric synaptic junctions (see Fig. 7*F*, arrowhead).

Taken together, these data demonstrate that E- and

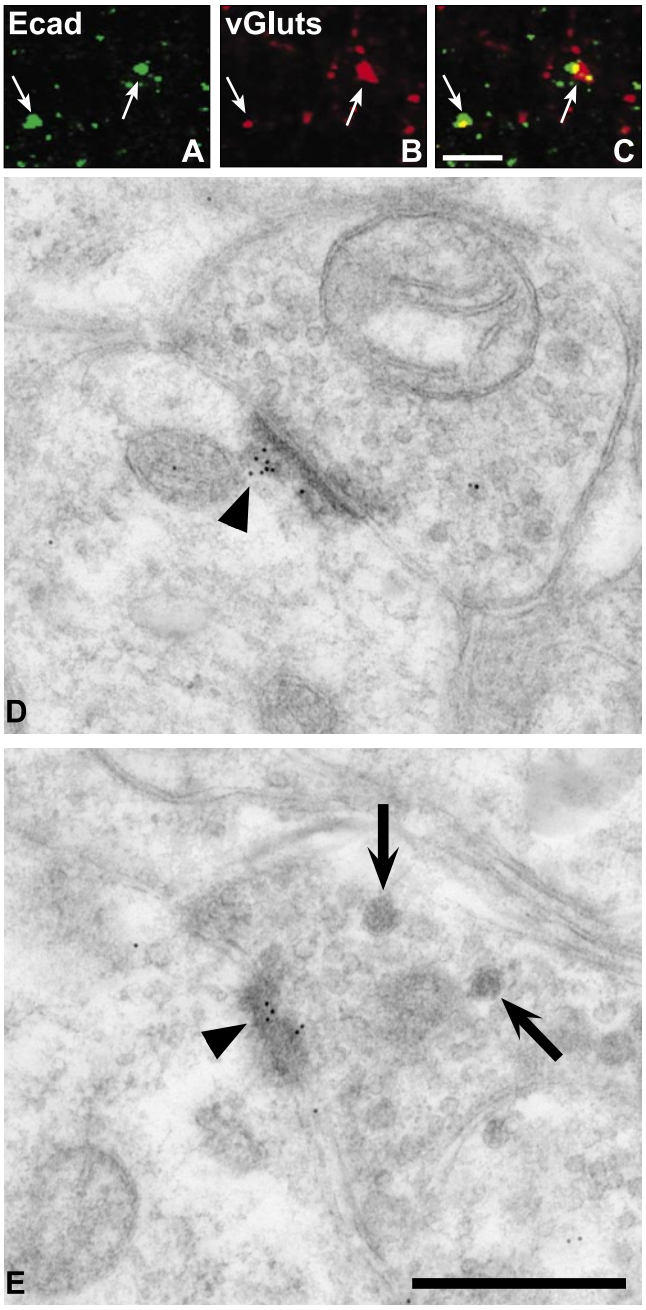

Figure 3. E-cadherin localizes to excitatory synaptic junctions within lamina IIi of the adult dorsal horn. Confocal images showing puncta immunolabeled for E-cadherin (*A*; green) and vGluts (*B*; red), separately and as an overlay (*C*; regions of yellow indicate codistribution). Arrows indicate identical puncta in each set of separate and overlaid images. *D*, *E*, Electron micrographs showing immunogold localization of E-cadherin antibody to asymmetric postsynaptic densities (arrowheads). Large dense-core vesicles (arrows) can be seen in the terminal shown in *E*. Scale bars: *A–C*, 5 μm; *D*, *E*, 500 nm.

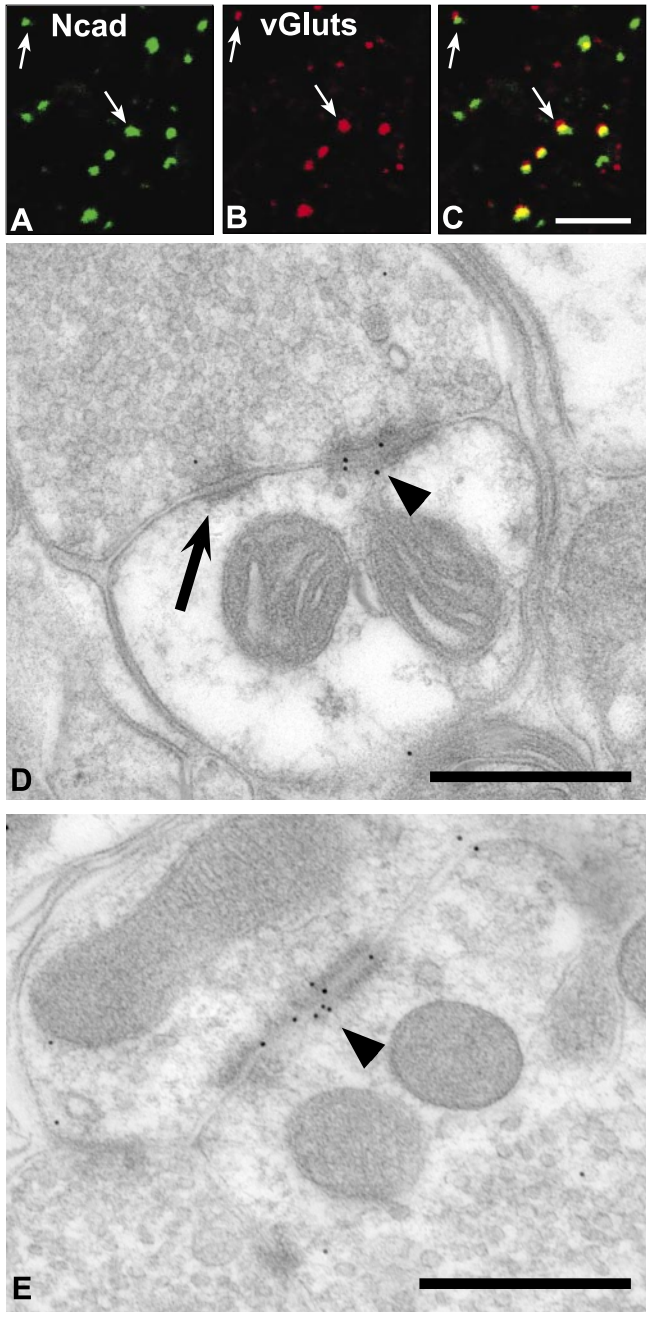

Figure 4. N-cadherin localizes to excitatory synaptic junctional complexes within lamina IIo of the adult dorsal horn. Confocal images showing puncta immunolabeled for N-cadherin (*A*; green) and vGluts (*B*; red), separately and as an overlay (*C*; regions of yellow indicate codistribution). Arrows indicate identical puncta in each set of separate and overlaid images. *D*, *E*, Electron micrographs showing immunogold localization of rabbit N-cadherin antibody to a punctum adherens junction (*D*; arrowhead) adjacent to a conventional asymmetric postsynaptic density that lacks gold particles (*D*; arrow). N-cadherin antibody binding was also localized to some axoaxonic synapses (*E*; arrowhead). Scale bars: *A–C*, 5 μm; *D*, *E*, 500 nm.

N-cadherin localize to excitatory synaptic junctional complexes in spinal dorsal horn.

Identity of E- and N-cadherin-associated synaptic circuitry within dorsal horn

The partially overlapping but distinct laminar distributions of the two cadherins, coupled with their synaptic localization, raised the possibility that each might be found in association with different functional types of spinal synapses, similar to the synaptic specificity they display in the brain (Huntley et al., 2002). To investigate this, we used a triple-immunolabeling strategy, combining well established markers of different primary afferent and intrinsic circuits with presynaptic terminal markers and cadherin labeling (see Materials and Methods for more details). The results of this quantitative analysis are shown in Table 1.

We first examined cadherin affiliation with the synaptic terminations of small-diameter primary sensory afferents (unmyelinated C-fibers and thinly myelinated A∂-fibers) through which

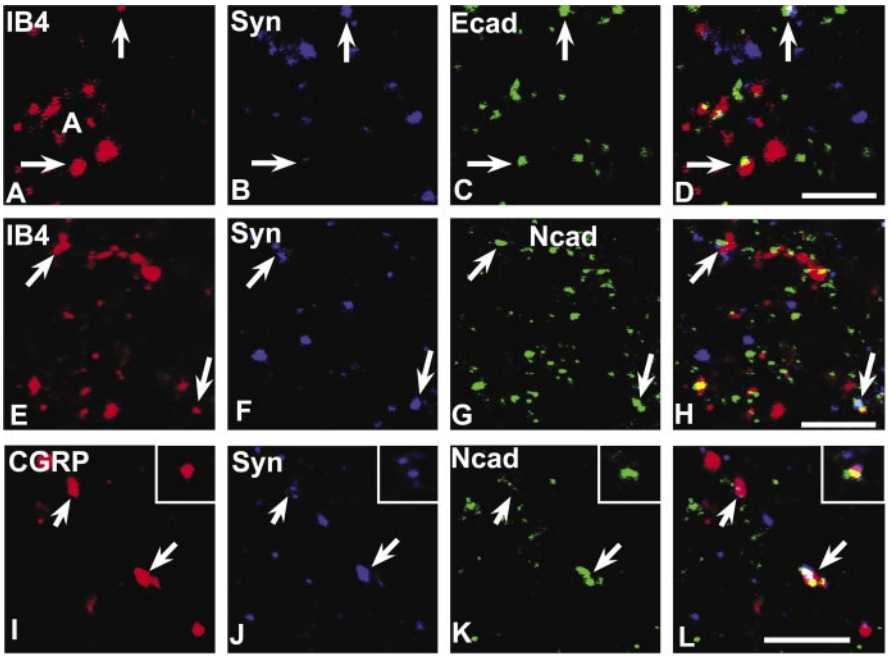

Figure 5. E- and N-cadherin codistribute with markers of primary afferent C-fiber synapses in lamina II. The nonpeptidergic C-fiber afferents to lamina IIi are labeled by IB4 binding (*A*, *E*), whereas the peptidergic C-fiber afferents to lamina IIo are labeled by CGRP (*I*); those forming synaptic terminals are identified by synaptophysin colabeling (*B*, *F*, *J*), and many of these contain E-cadherin (*C*) or N-cadherin (*G*, *K*), shown separately and in the overlays (*D*, *H*, *L*; regions of white indicate codistribution of all three labels). Insets in *I–L* show a representative example of a peptidergic C-fiber synaptic punctum containing N-cadherin. Scale bars, 5 μm.

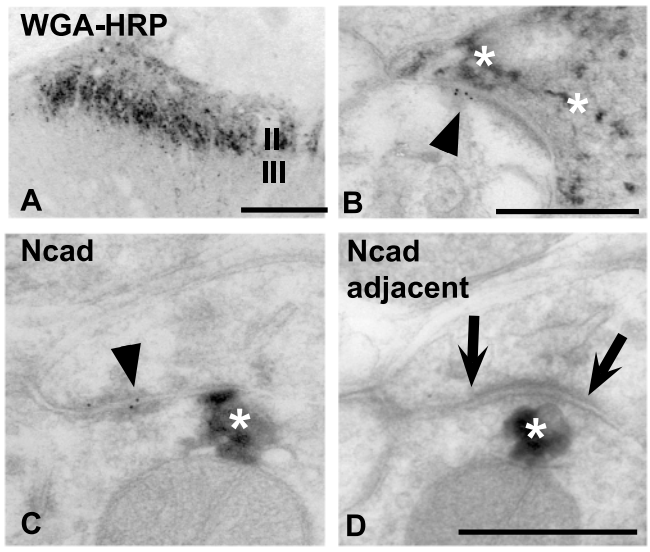

Figure 6. Immunogold electron microscopic localization of E- and N-cadherin at synaptic junctions formed by WGA–HRP-identified primary afferents in lamina II. *A*, Low-power, light microscopic image through lumber dorsal horn showing typical lamina II termination pattern of small-diameter, myelinated, and unmyelinated primary afferents. TMB histochemistry was used to reveal such terminals after selective uptake and transganglionic transport of WGA–HRP injected into the sciatic nerve. Medial is to the right. *B*, Electron micrograph of C-fiber synapse in lamina IIi. E-cadherin antibody binding (arrowhead) is localized to an asymmetric postsynaptic density. The presynaptic terminal is identified as a small-diameter (nociceptive) afferent because it contains TMB reaction product (asterisks). *C*, *D*, Serial electron micrographs through a C-fiber synapse in lamina IIi immunogold-labeled for mouse N-cadherin antibody binding. Gold particles are found at perisynaptic puncta adherens (*C*; arrowhead) but are absent from the conventional asymmetric synaptic junction that is seen in the immediately adjacent section (Ncad adjacent; *D*; arrows). Asterisks in *C* and *D* indicate TMB reaction product contained in the afferent terminal. Scale bars: *A*, 100 μm; *B–D*, 500 nm.

nociceptive information is conveyed to lamina II. These are composed of nonpeptidergic and peptidergic subtypes. The former can be identified by labeling for IB4 binding and terminate in lamina IIi (Alvarez et al., 1991; Kitchener et al., 1994). The latter can be identified by labeling for CGRP and terminate in laminas I–IIo (Alvarez et al., 1991).

The vast majority of the IB4–synaptophysin-positive puncta (~80%) (Table 1) in lamina IIi codistributes with E-cadherin (Fig. 5*A–D*), whereas only a minority of these (~9%) codistribute with N-cadherin (Fig. 5*E–H*). We also found many E- or N-cadherin–IB4 puncta that lacked synaptophysin labeling, but their numbers relative to those that were synaptic were not quantified. Such nonsynaptic codistribution may correspond to a previous observation that E-cadherin immunoreactivity is present along fasciculated, small-diameter axons (Seto et al., 1997). In contrast, a majority (~65%) of the CGRP–synaptophysin-positive puncta in lamina IIo codistribute with N-cadherin (Fig. 5*I–L*). E-cadherin codistribution with CGRP was not examined because there is virtually no E-cadherin label in lamina IIo. Together, the data suggest that between these two cadherins, E-cadherin is preferentially associated with terminations of nonpeptidergic nociceptive afferents, whereas N-cadherin is preferentially associated with terminations of peptidergic nociceptive afferents.

To verify cadherin localization to the principal synaptic relay that conveys pain information, we combined intrasciatic nerve injections of WGA–HRP with cadherin immunogold electron microscopy. WGA–HRP is selectively taken up by C- and A∂-fibers and transported transganglionically to their spinal terminations in laminas I–II (LaMotte et al., 1991; Kitchener et al., 1994), which we confirmed (Fig. 6*A*). As predicted, E-cadherin gold particles are found at asymmetric synapses (Fig. 6*B*, arrowhead) where the presynaptic terminal is filled with WGA–HRP histochemical reaction product (Fig. 6*B*, asterisks). N-cadherin gold particles are also found at synaptic junctional complexes associated with presynaptic terminals containing WGA–HRP reaction product (Fig. 6*C*,*D*, asterisk). However, such gold clusters are found at puncta adherens (Fig. 6*C*, arrowhead), immediately adjacent to conventional asymmetric synaptic junctions that lack gold particles (Fig. 6*D*, arrows). Technical limitations prevented us from examining whether E- and N-cadherin colocalize to the same WGA–HRP (or any other) labeled terminals.

We next investigated cadherin association with the terminations of large-diameter, myelinated Aβ-fibers conveying low-threshold mechanosensation to laminas III–V. These afferent terminations are labeled selectively by intrasciatic nerve injections of CTB conjugates (LaMotte et al., 1991), which we verified (Fig. 7*E*). Quantitatively, ~50% of the CTB–vGlut-positive puncta in lamina III codistribute with labeling for N-cadherin (Table 1; Fig. 7*A–D*). Synaptic association was verified by immunogold electron microscopy, in which N-cadherin gold particles are found at asymmetric synapses (Fig. 7*F*, arrowhead) in which the presynaptic terminal is filled with CTB–HRP reaction product (Fig. 7*F*,

asterisk). E-cadherin was not evaluated in relationship to this projection because Aβ-fibers terminate deep to lamina IIi in which E-cadherin is found.

Finally, we examined cadherin association with two representative intrinsic systems. NT labels a population of intrinsic excitatory neurons and their terminals in lamina II (Todd and Spike, 1993). A smaller percentage of NT–vGlut-positive synapses in lamina IIi (Fig. 8*A–D*) are E-cadherin labeled (~30%) (Table 1) in comparison with those that are N-cadherin labeled (~50%) (Fig. 8*E–H*). GAD labels a population of synaptic terminals furnished by intrinsic interneurons that use the inhibitory neurotransmitter GABA (Ribak et al., 1978). Both E- and N-cadherin labeling are found associated with some GAD-positive puncta (Fig. 8*I–N*). Quantitatively, E- and N-cadherin are associated with an equal percentage (~30%) of GAD-positive inhibitory synaptic puncta in lamina IIi. These data are of interest because in brain, GABAergic synapses contain catenins but lack N-cadherin; the corresponding cadherins have not yet been identified (Yamagata et al., 1995; Benson and Tanaka, 1998; Huntley and Benson, 1999).

To summarize, these data demonstrate that E- and N-cadherin are localized to differential proportions of functionally distinct primary afferent and intrinsic synaptic circuits in the dorsal horn. Such localization patterns are complex; none of the various markers that we used to identify different primary afferent or intrinsic systems was associated exclusively with E- or N-cadherin. It may be that within any given system defined by fiber or neurotransmitter type, one or a few cadherins will delineate subpopulations of synapses that are functionally related. For example, Aβ-fibers convey information from different types of peripheral sensory receptors (Brown and Iggo, 1967). It is possible that the Aβ-fiber synapses that we found associated with N-cadherin (~50%) represent a submodality-specific subpopulation; which cadherin (if any) is present at those that lack N-cadherin remains to be determined.

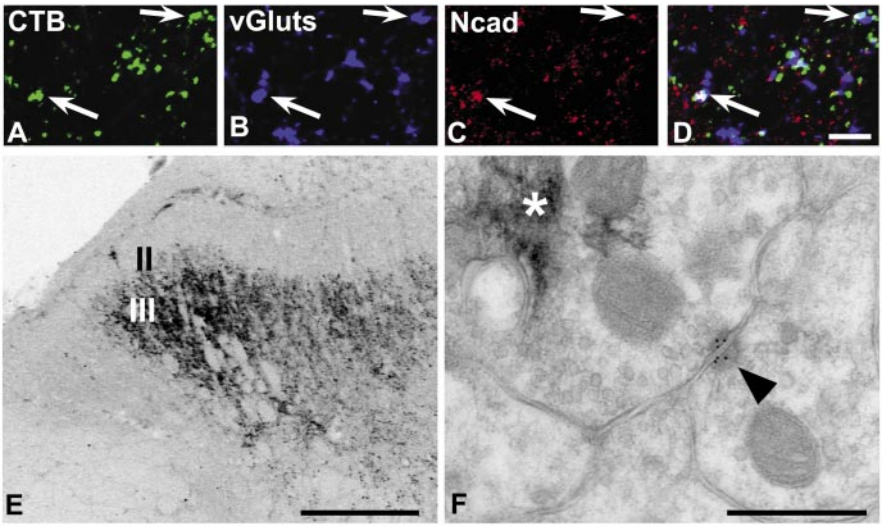

Figure 7. N-cadherin localizes to Aβ-fiber synapses in lamina III. The terminations of Aβ-fibers were identified by transganglionic transport of CTB conjugates injected into the sciatic nerve. *A–D*, Confocal images showing puncta (arrows) containing CTB–Alexa 488 (*A*; green) immunolabeled for the synaptic marker vGluts (*B*; blue) and N-cadherin (*C*; red), separately and as an overlay (*D*; regions of white indicate codistribution of all three labels). *E*, Low-power, light microscopic image through lumber dorsal horn showing typical lamina III termination pattern of large-diameter, myelinated Aβ-fiber primary afferents revealed by CTB–HRP transport and TMB histochemistry. *F*, Electron micrograph of Aβ-fiber synapse in lamina III. Rabbit N-cadherin antibody binding is localized to an asymmetric synaptic contact (arrowhead). TMB reaction product (asterisk) is contained within the presynaptic terminal. Scale bars: *A–D*, 5 μm; *E*, 100 μm; *F*, 500 nm.

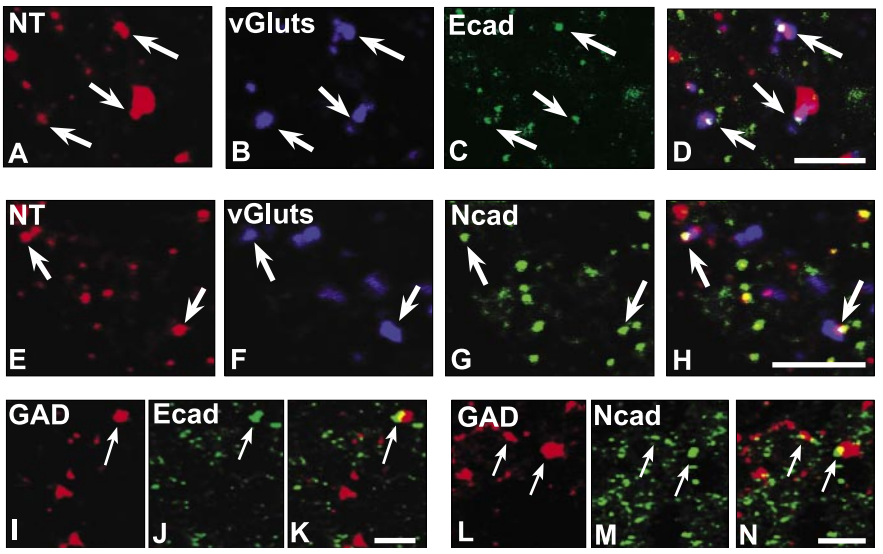

Figure 8. E- and N-cadherin localize to excitatory and inhibitory synapses of intrinsic origin in lamina II. Confocal images of intrinsic excitatory synaptic puncta identified by labeling for NT (*A*, *E*; red), vGluts (*B*, *F*; blue), and E-cadherin (*C*; green) or N-cadherin (*G*; green) are shown separately and as overlays (*D*, *H*; regions of white indicate codistribution of all three markers). Confocal images of intrinsic inhibitory synaptic puncta identified by codistribution of labeling for GAD (*I*, *L*; red) and E- cadherin (*J*; green) or N-cadherin (*M*; green) are shown separately and as overlays (*K*, *N*; regions of yellow indicate codistribution). Scale bars, 5 μm.

Peripheral nerve injury differentially affects levels and localization of cadherins

Neuropathic pain is associated with peripheral nerve injury; mechanical hyperalgesia and autotomy are apparent by ~10–21 d after sciatic nerve axotomy (Kingery and Vallin, 1989; Kauppila and Xu, 1996). Structural synaptic reorganization of dorsal horn primary afferent circuitry is thought to contribute, in part, to such maladapative behavior (Knyihar and Csillik, 1976; Woolf et al., 1992), raising the possibility that cadherin adhesive function or localization is affected under such conditions. To investigate this, we first verified that unilateral sciatic nerve axotomy produced dorsal horn neurochemical changes that have been associated previously with this type of injury. As expected, by 7 d after axotomy and thereafter, spinal sections through the lumbar (L4/L5) dorsal horn from these animals display the characteristic loss of IB4 binding in lamina IIi within the sciatic nerve termination territory (Figs. 9*A*, 10*A*; arrows) as described previously (Molander et al., 1996). We next examined cadherin immunolocalization in lumbar dorsal horn at staggered intervals after sciatic

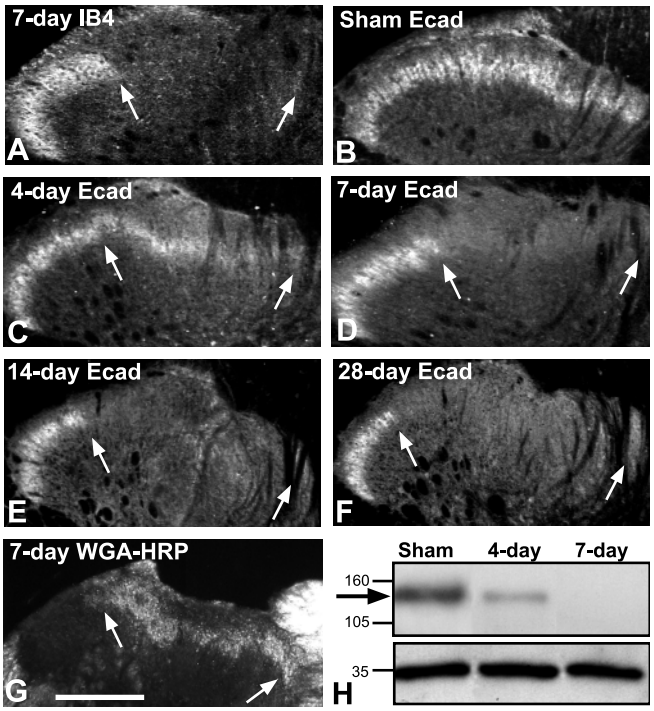

Figure 9. Rapid and complete loss of E-cadherin after sciatic nerve axotomy. In all images, the region between arrows corresponds to the sciatic nerve termination zone in lamina IIi. *A*, IB4 binding is completely lost from the sciatic nerve termination zone by 7 d after axotomy but remains as expected more laterally in the region corresponding to saphenous nerve terminations. *B–F*, Fluorescence photomicrographs showing E-cadherin labeling in lamina IIi. A normal pattern of immunolabel is seen in the sham-operated control side (*B*). Intensity of immunolabel diminishes at 4 d after axotomy (*C*) and is undetectable in the sciatic nerve termination zone (arrows) by 7 d after axotomy (*D*). The loss of E-cadherin persists at 14 d (*E*) and at 28 d after axotomy (*F*). Sections shown in *A*, *B*, and *D* are from the same animal. *G*, Dark-field photomicrograph showing mostly normal pattern of TMB-reacted WGA–HRP terminal transport to lamina IIi after sciatic nerve axotomy. WGA–HRP was injected 4 d after axotomy and killed 3 d later. *H*, Representative E-cadherin immunoblot of extracts of lamina I/II taken from indicated conditions and days after sciatic nerve axotomy. The arrow indicates the position of bands corresponding to E-cadherin. E-cadherin levels are diminished by 4 d and completely absent by 7 d after axotomy, matching the post-axotomy patterns of immunolabeling. The bottom bands correspond to GAPDH, used as a loading control. Medial is to the right in *A–G*. Scale bars: *A–G*, 100 μm.

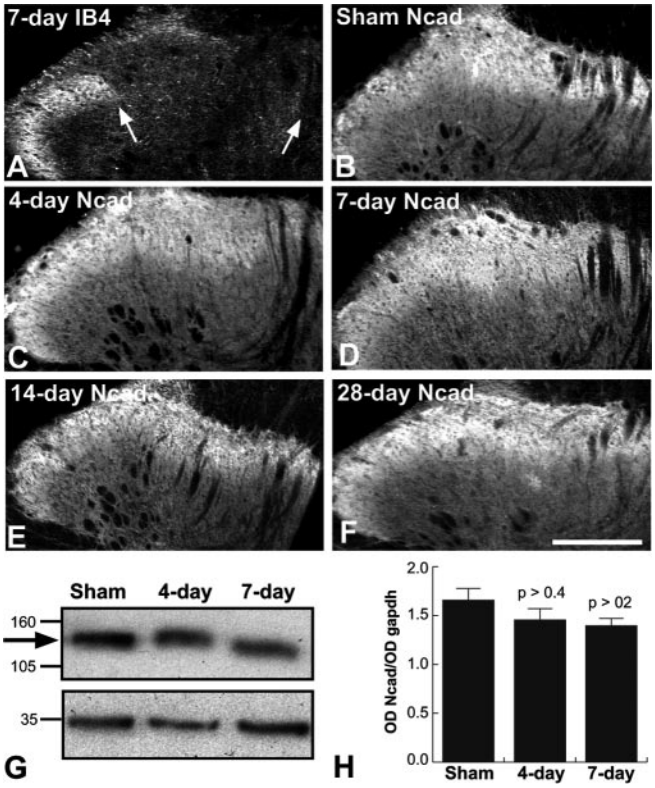

Figure 10. N-cadherin protein levels and localization unaltered by sciatic nerve axotomy. *A*, IB4 binding at 7 d after axotomy is completely absent from the sciatic nerve termination zone (between arrows), as expected. *B–F*, Fluorescence photomicrographs showing N-cadherin labeling throughout laminas I–III. Normal patterns and intensity of immunolabel are seen in sham-operated (*B*) and lesioned (*C–F*) animals at each post-axotomy time point examined (4, 7, 14, and 28 d). Sections shown in *A*, *B*, and *D* are from the same animal. Medial is to the right in *A–F*. *G*, Representative N-cadherin immunoblot of extracts of lamina I/II taken from indicated conditions and days after sciatic nerve axotomy. The arrow indicates the position of bands corresponding to N-cadherin. The bottom bands correspond to GAPDH, used as a loading control. *H*, Densitometric time course analysis shows N-cadherin protein levels do not change significantly with sciatic nerve axotomy. Data are means + SEM of ratios of N-cadherin band intensity to GAPDH band intensity (OD Ncad/OD gapdh). Each *p* value corresponds to comparison between relevant lesion group and sham control group. Scale bar, *A–F*, 100 μm.

nerve axotomy. At 1 d after axotomy, there are no changes in the pattern of E-cadherin immunolocalization in lamina IIi in comparison with sham-operated or unoperated control animals. However, at 4 d after axotomy, E-cadherin immunofluorescence is diminished within the sciatic nerve termination zone on the lesioned side (Fig. 9*C*, arrows) in comparison with sham-operated controls (Fig. 9*B*). At 7 d after axotomy, E-cadherin immunolabeling is undetectable within the sciatic nerve termination zone (Fig. 9*D*, arrows) but remains as expected in the laterally adjacent zone of uninjured saphenous nerve terminations. Injection of WGA–HRP into the sciatic nerve at 4 d after axotomy reveals a mostly normal pattern of terminal fiber labeling within lamina II when examined at 7 d after axotomy (Fig. 9*G*), indicating that such loss of E-cadherin immunolabeling observed is not likely attributable to significant loss of primary afferent fibers. The complete absence of E-cadherin immunolabeling within the sciatic nerve termination zone is still evident at 14 d after axotomy (Fig. 9*E*) and persists through at least 28 d after axotomy (Fig. 9*F*), the latest time point that we examined in the study. Immunoblots of tissue-punches through the sciatic nerve termination territory show levels of E-cadherin that are diminished at 4 d after axotomy in comparison with sham controls, becoming undetectable by 7 d after axotomy (Fig. 9*H*). Taken together, these data indicate that the progressive loss of E-cadherin immunofluoresence in lamina IIi is likely attributable to the gradual reduction in protein levels in the absence of overt loss of primary afferent fibers or parent DRG neurons.

In contrast to the progressive loss of E-cadherin, there is no apparent effect on the immunolocalization pattern of N-cadherin in the dorsal horn after sciatic nerve injury during the same post-axotomy period examined (1–28 d) (Fig. 10*B–F*). Quantitative immunoblot analysis of dorsal horn tissue punches confirms that there are no significant changes in levels of N-cadherin in comparison with sham-operated controls (Fig. 10*G*,*H*).

Taken together, these data demonstrate that levels and localization of two synaptic cadherins are differentially affected by peripheral nerve injury.

Discussion

We show that E- and N-cadherin are parceled to different proportions of functionally, anatomically and neurochemically distinct types of synaptic and other junctions of intrinsic and pri-

mary afferent origin in adult rat spinal dorsal horn. Such specificity is particularly evident in the distribution of the two cadherins in relationship to the terminations of unmyelinated primary afferent C-fibers that convey pain information to lamina II. Nonpeptidergic C-fiber synapses in lamina IIi contain E-cadherin but mostly lack N-cadherin, whereas the majority of the peptidergic C-fiber synapses in lamina IIo contain N-cadherin but lack E-cadherin. Additionally, the distribution and levels of the two cadherins are differentially affected by sciatic nerve axotomy, a model of neuropathic pain in which structural and functional reorganization of the dorsal horn has been implicated (Csillik and Knyihar, 1975; Devor and Wall, 1981; Kapadia and LaMotte, 1987; Woolf et al., 1992). E-cadherin is rapidly lost from the dorsal horn synapses with which it is affiliated, whereas N-cadherin localization and levels are unchanged; such patterns persist at least through 28 d postlesion. The loss of E-cadherin thus occurs before any detectable onset of mechanical hyperalgesia (~10–21 d after axotomy), as reported previously (Kingery and Vallin, 1989; Kauppila and Xu, 1996). The synaptic specificity displayed by these cadherins, coupled with their differential response to injury, suggests that they may proactively contribute to the maintenance of some, and incipient dismantling of other, synaptic circuits in response to nerve injury. Speculatively, such changes may ultimately contribute to subsequently emerging abnormalities in pain perception.

Our results demonstrate that classic cadherins are an integral component of the mature synaptic junctional complex in spinal cord. Immunogold localization of cadherin/catenin proteins at brain synapses suggests that N-cadherin and their catenin-binding partners are clustered at perisynaptic puncta adherens adjacent to the transmitter release zone (Uchida et al., 1996). Clustered N-cadherin labeling has also been observed at the edges of or along some postsynaptic densities in direct apposition to the transmitter release zone (Yamagata et al., 1995; Fannon and Colman, 1996; Bozdagi et al., 2000). In our adult spinal dorsal horn material, we saw evidence for both synaptic and perisynaptic distribution. Such subsynaptic parcelation at lamina II synapses may be cadherin type specific, although this is suggested cautiously because our sampling was limited. In our material, E-cadherin was associated mostly with conventional asymmetric synapses, whereas N-cadherin was associated mostly with perisynaptic puncta adherens. The significance of such differential parcelation is presently unknown. It is possible that E- and N-cadherin delineate subpopulations of lamina II synapses or synaptic complexes, the adhesive integrity, and therefore structural stability, of which differs in the face of peripheral nerve injury. It is unlikely that the loss of E-cadherin reflects overt neuron loss, because neuron death in DRG or cord or loss of unmyelinated axons within dorsal roots is virtually nonexistent over the time course of our studies (Sugimoto and Gobel, 1982; Coggeshall et al., 1997, 2001; Tandrup et al., 2000). Furthermore, we observed a normal laminar pattern of WGA–HRP labeling at 7 d after axotomy, which would not be expected if significant numbers of DRG neurons were dying. That significant loss of E-cadherin was already detectable by 4 d after axotomy suggests instead that such loss represents one of the earliest molecular changes indicative of incipient synaptic structural dissolution and reorganization of the neuropil. Ultrastructurally, the terminals of nonpeptidergic C-fiber afferents to lamina II undergo signs of terminal degeneration and engulfment by glial processes after sciatic nerve injury, with a time course identical to the rapid loss of E-cadherin that we observed here (Coimbra et al., 1974; Knyihar and Csillik, 1976; Kapadia and LaMotte, 1987). The mechanisms for such loss could include transcriptional downregulation of E-cadherin or directed extracellular cleavage of the E-cadherin ectodomain via matrix metalloproteinases, which are upregulated by spinal or nerve injury (de Castro et al., 2000; Komori et al., 2004). In epithelial cells, matrix metalloproteinases can clip the E-cadherin ectodomain, leading to the dismantling of puncta adherens (Lochter et al., 1997; Steinhusen et al., 2001; Marambaud et al., 2002). Intracellularly orchestrated uncoupling of the E-cadherin-catenin linkage to the actin cytoskeleton could also occur, which would also greatly diminish or abolish adhesive force (Nagafuchi and Takeichi, 1988). This could occur either by downregulation of catenins (Seto et al., 1997) or through catenin phosphorylation, which negatively regulates cadherin–catenin association (Roura et al., 1999). Thus, the loss of E-cadherin-mediated adhesion between apposed synaptic or other membranes may represent the first in a series of molecular cascades that lead ultimately to the loss of the synaptic junctions themselves.

Interestingly, the loss of E-cadherin may also have included synaptic contacts furnished by axon terminals of intrinsic neurons, and therefore not directly injured, such as those containing GABA or NT. In hippocampal neurons, synaptic activity regulates N-cadherin synthesis, localization, molecular configuration, and affiliation with catenins (Bozdagi et al., 2000; Tanaka et al., 2000; Murase et al., 2002). Thus, the aberrant patterns of afferent activity resulting from nerve injury (Laird and Bennett, 1993; Xie et al., 1995; Kohno et al., 2003) could lead to activity-dependent downregulation of E-cadherin expression within such intrinsic neuron populations, similar to the reported loss of GAD or other molecules after nerve injury (Dubner and Ruda, 1992; Castro-Lopes et al., 1993). In our material, the loss of E-cadherin persisted through 28 d after axotomy, the latest post-injury time we examined. Whether E-cadherin expression returns at time points later than this, perhaps as new nonpeptidergic afferents or some other fiber systems sprout (LaMotte et al., 1989; Doubell and Woolf, 1997; Blomqvist and Craig, 2000; Darian-Smith, 2004), remains to be determined. Under different injury conditions (nerve crush), immunoreactivity for E-cadherin and α-N-catenin reappears ~2 months later (Seto et al., 1997).

Although the time course of E-cadherin loss correlates well with the reported onset of terminal degeneration as discussed above, they both occur earlier than detectable abnormalities in pain sensation. Thus, it is possible that the loss of E-cadherin and any related structural changes to the primary afferent synapses with which it is affiliated are not directly related to subsequently developing neuropathic pain. As emphasized recently (Light and Perl, 2003), it is often overlooked that a significant contingent of C-fiber afferents to lamina II convey innocuous mechanoreception. Many such afferents terminate deep to those that convey nociception (Light and Perl, 1979; Sugiura et al., 1986), suggesting that these may correspond to some of the E-cadherin-affiliated primary afferent synapses in lamina IIi. Their loss could therefore be unrelated to the later onset of neuropathic pain. In contrast, mechanical nociceptive thresholds are elevated in rats subjected to targeted deletion of the IB4-binding population of small DRG neurons (Vulchanova et al., 2001). This suggests that the loss of E-cadherin and any associated structural changes to IB4-positive circuitry that starts very early may eventually contribute to the later-appearing mechanical allodynia that accompanies nerve-cut lesion, perhaps by a progressive accumulation of synapse loss or reorganization until some threshold is surpassed.

The unchanging pattern of N-cadherin labeling after nerve

injury suggests that the primary afferent and intrinsic synapses with which N-cadherin is affiliated are stable and resistant to degenerative changes over the same period that E-cadherin is lost. This is consistent with observations that functionally, synaptic transmission of such peptidergic circuits are intimately involved in conveying stimuli that are perceived aberrantly as painful (Schaible, 1996). Intrathecal injection of CGRP, for example, leads to tactile allodynia and thermal hypersensitivity in the absence of any overt nerve injury (Sun et al., 2003). Speculatively, such stability may reflect the presence within these synaptic complexes of the perisynaptic N-cadherin labeled puncta adherens, which are classically recognized, strongly adhesive contact sites that contain, in addition to cadherins (Yap et al., 1997), adhesion proteins of the Ig superfamily such as nectins and afadins (Mandai et al., 1997; Nishioka et al., 2000). In our material, we found that ~65% of the peptidergic afferents contained N-cadherin. It is not clear at present whether the remaining ~35% lack N-cadherin because they also lack perisynaptic puncta adherens. If this is the case, then perhaps it would be expected that such peptidergic afferent synapses would also degenerate after axotomy, similar to E-cadherin-affiliated synapses. This might explain the reported diminishment in intensity of CGRP immunolabeling within lamina IIo after sciatic nerve injury (Groves et al., 1996). It remains to be determined whether N-cadherin levels eventually change over time courses later than 28 d after injury, but it is unlikely because there is little evidence ultrastructurally for any remaining terminal degeneration in lamina II 14 d after axotomy (Arvidsson et al., 1986).

One of the prevailing models for tactile allodynia after nerve injury invokes sprouting of large-diameter mechanoreceptive Aβ-fibers from their normal terminations in lamina III into lamina II, where they form new, aberrantly targeted synapses (Woolf et al., 1992, 1995; Kohama et al., 2000). N-cadherin is a potent substrate for axonal growth and laminar targeting developmentally (Bixby and Zhang, 1990; Poskanzer et al., 2003), and in adult epilepsy models in which hippocampal mossy fibers sprout, N-cadherin mRNA and protein levels are dramatically upregulated, with *de novo* N-cadherin immunoreactivity strongly delineating the mossy fiber sprouts (Shan et al., 2002). The lack of any demonstrable changes in N-cadherin levels or patterns of localization after sciatic nerve axotomy are inconsistent with such overt sprouting and instead support, albeit indirectly, recent studies that have challenged the Aβ-fiber-sprouting model on other, more direct grounds (Tong et al., 1999; Bao et al., 2002; Hughes et al., 2003; Shehab et al., 2003). Alternatively, the lack of any changes in N-cadherin may be because Aβ-fibers use molecules other than N-cadherin for growth under conditions of injury-induced sprouting (Zhang et al., 1998).

References

Alvarez FJ, Morris HR, Priestley JV (1991) Sub-populations of smaller diameter trigeminal primary afferent neurons defined by expression of calcitonin gene-related peptide and the cell surface oligosaccharide recognized by monoclonal antibody LA4. J Neurocytol 20:716–731.

Arndt K, Nakagawa S, Takeichi M, Redies C (1998) Cadherin-defined segments and parasagittal cell ribbons in the developing chicken cerebellum. Mol Cell Neurosci 10:211–228.

Arvidsson J, Ygge J, Grant G (1986) Cell loss in lumbar dorsal root ganglia and transganglionic degeneration after sciatic nerve resection in the rat. Brain Res 373:15–21.

Bao L, Wang HF, Cai HJ, Tong YG, Jin SX, Lu YJ, Grant G, Hokfelt T, Zhang X (2002) Peripheral axotomy induces only very limited sprouting of coarse myelinated afferents into inner lamina II of rat spinal cord. Eur J Neurosci 16:175–185.

Benson DL, Tanaka H (1998) N-cadherin redistribution during synaptogenesis in hippocampal neurons. J Neurosci 18:6892–6904.

Bixby JL, Zhang R (1990) Purified N-cadherin is a potent substrate for the rapid induction of neurite outgrowth. J Cell Biol 110:1253–1260.

Blomqvist A, Craig AD (2000) Is neuropathic pain caused by the activation of nociceptive-specific neurons due to anatomic sprouting in the dorsal horn? [In Process Citation]. J Comp Neurol 428:1–4.

Bozdagi O, Shan W, Tanaka H, Benson DL, Huntley GW (2000) Increasing numbers of synaptic puncta during late-phase LTP: N-cadherin is synthesized, recruited to synaptic sites, and required for potentiation. Neuron 28:245–259.

Brown AG, Iggo A (1967) A quantitative study of cutaneous receptors and afferent fibres in the cat and rabbit. J Physiol (Lond) 193:707–738.

Castro-Lopes JM, Tavares I, Coimbra A (1993) GABA decreases in the spinal cord dorsal horn after peripheral neurectomy. Brain Res 620:287–291.

Cervero F, Iggo A (1980) The substantia gelatinosa of the spinal cord: a critical review. Brain 103:717–772.

Chaudhry FA, Lehre KP, van Lookeren Campagne M, Ottersen OP, Danbolt NC, Storm-Mathisen JG (1995) Glutamate transporters in glial plasma membranes: highly differentiated localizations revealed by quantitative ultrastructural immunocytochemistry. Neuron 15:711–720.

Coggeshall RE, Lekan HA, Doubell TP, Allchorne A, Woolf CJ (1997) Central changes in primary afferent fibers following peripheral nerve lesions. Neuroscience 77:1115–1122.

Coggeshall RE, Lekan HA, White FA, Woolf CJ (2001) A-fiber sensory input induces neuronal cell death in the dorsal horn of the adult rat spinal cord. J Comp Neurol 435:276–282.

Coimbra A, Sodre-Borges BP, Magalhaes MM (1974) The substantia gelatinosa Rolandi of the rat. Fine structure, cytochemistry (acid phosphatase) and changes after dorsal root section. J Neurocytol 3:199–217.

Csillik B, Knyihar E (1975) Degenerative atrophy and regenerative proliferation in the rat spinal cord. Z Mikrosk Anat Forsch 89:1099–1103.

Darian-Smith C (2004) Primary afferent terminal sprouting after a cervical dorsal rootlet section in the macaque monkey. J Comp Neurol 470:134–150.

de Castro Jr RC, Burns CL, McAdoo DJ, Romanic AM (2000) Metalloproteinase increases in the injured rat spinal cord. NeuroReport 11:3551–3554.

Devor M, Wall PD (1981) Plasticity in the spinal cord sensory map following peripheral nerve injury in rats. J Neurosci 1:679–684.

Doubell TP, Woolf CJ (1997) Growth-associated protein 43 immunoreactivity in the superficial dorsal horn of the rat spinal cord is localized in atrophic C-fiber, and not in sprouted A-fiber, central terminals after peripheral nerve injury. J Comp Neurol 386:111–118.

Dubner R, Ruda MA (1992) Activity-dependent neuronal plasticity following tissue injury and inflammation. Trends Neurosci 15:96–103.

Fannon AM, Colman DR (1996) A model for central synaptic junctional complex formation based on the differential adhesive specificities of the cadherins. Neuron 17:423–434.

Fredette BJ, Ranscht B (1994) T-cadherin expression delineates specific regions of the developing motor axon-hindlimb projection pathway. J Neurosci 14:7331–7346.

Geiger B, Ayalon O (1992) Cadherins. Annu Rev Cell Biol 8:307–332.

Gil OD, Needleman L, Huntley GW (2002) Developmental patterns of cadherin expression and localization in relation to compartmentalized thalamocortical terminations in rat barrel cortex. J Comp Neurol 453:372–388.

Groves MJ, Ng YW, Ciardi A, Scaravilli F (1996) Sciatic nerve injury in the adult rat: comparison of effects on oligosaccharide, CGRP and GAP43 immunoreactivity in primary afferents following two types of trauma. J Neurocytol 25:219–231.

Hjelle OP, Chaudhry FA, Ottersen OP (1994) Antisera to glutathione: characterization and immunocytochemical application to the rat carebellum. Eur J Neurosci 6:794–804.

Horner PJ, Gage FH (2000) Regenerating the damaged central nervous system. Nature 407:963–970.

Hughes DI, Scott DT, Todd AJ, Riddell JS (2003) Lack of evidence for sprouting of Aβ afferents into the superficial laminas of the spinal cord dorsal horn after nerve section. J Neurosci 23:9491–9499.

Huntley GW (2002) Dynamic aspects of cadherin-mediated adhesion in synapse development and plasticity. Biol Cell 94:335–344.

Huntley GW, Benson DL (1999) N-Cadherin at developing thalamocortical synapses provides an adhesion mechanism for the formation of somatotopically organized connections. J Comp Neurol 407:453–471.

Huntley GW, Gil O, Bozdagi O (2002) The cadherin family of cell adhesion molecules: multiple roles in synaptic plasticity. Neuroscientist 8:221–233.

Inoue A, Sanes JR (1997) Lamina-specific connectivity in the brain: regulation by N-cadherin, neurotrophins, and glycoconjugates. Science 276:1428–1431.

Kapadia SE, LaMotte CC (1987) Deafferentation-induced alterations in the rat dorsal horn: I. Comparison of peripheral nerve injury vs. rhizotomy effects on presynaptic, postsynaptic, and glial processes. J Comp Neurol 266:183–197.

Kauppila T, Xu XJ (1996) Sciatic nerve section induces mechanical hyperalgesia in skin adjacent to the deafferented region in rats: lack of correlation with autotomy behavior. Neurosci Lett 211:65–67.

Khasabov SG, Rogers SD, Ghilardi JR, Peters CM, Mantyh PW, Simone DA (2002) Spinal neurons that possess the substance P receptor are required for the development of central sensitization. J Neurosci 22:9086–9098.

Kingery WS, Vallin JA (1989) The development of chronic mechanical hyperalgesia, autotomy and collateral sprouting following sciatic nerve section in rat. Pain 38:321–332.

Kitchener PD, Lapiz MD, Wilson P, Snow PJ (1994) Transganglionic labelling of primary sensory afferents in the rat lumbar spinal cord: comparison between wheatgerm agglutinin and the I-B4 isolectin from Bandeiraea simplicifolia. J Neurocytol 23:745–757.

Knyihar E, Csillik B (1976) Effect of peripheral anatomy on the fine structure and histochemistry of the Rolando substance: degenerative atrophy of central processes of pseudounipolar cells. Exp Brain Res 26:73–87.

Koerber HR, Mirnics K, Brown PB, Mendell LM (1994) Central sprouting and functional plasticity of regenerated primary afferents. J Neurosci 14:3655–3671.

Kohama I, Ishikawa K, Kocsis JD (2000) Synaptic reorganization in the substantia gelatinosa after peripheral nerve neuroma formation: aberrant innervation of lamina II neurons by Aβ afferents. J Neurosci 20:1538–1549.

Kohno T, Moore KA, Baba H, Woolf CJ (2003) Peripheral nerve injury alters excitatory synaptic transmission in lamina II of the rat dorsal horn. J Physiol (Lond) 548:131–138.

Komori K, Nonaka T, Okada A, Kinoh H, Hayashita-Kinoh H, Yoshida N, Yana I, Seiki M (2004) Absence of mechanical allodynia and Abeta-fiber sprouting after sciatic nerve injury in mice lacking membrane-type 5 matrix metalloproteinase. FEBS Lett 557:125–128.

Laird JM, Bennett GJ (1993) An electrophysiological study of dorsal horn neurons in the spinal cord of rats with an experimental peripheral neuropathy. J Neurophysiol 69:2072–2085.

LaMotte CC, Kapadia SE, Kocol CM (1989) Deafferentation-induced expansion of saphenous terminal field labelling in the adult rat dorsal horn following pronase injection of the sciatic nerve. J Comp Neurol 288:311–325.

LaMotte CC, Kapadia SE, Shapiro CM (1991) Central projections of the sciatic, saphenous, median, and ulnar nerves of the rat demonstrated by transganglionic transport of choleragenoid- HRP (B-HRP) and wheat germ agglutinin-HRP (WGA-HRP). J Comp Neurol 311:546–562.

Li JL, Fujiyama F, Kaneko T, Mizuno N (2003) Expression of vesicular glutamate transporters, VGluT1 and VGluT2, in axon terminals of nociceptive primary afferent fibers in the superficial layers of the medullary and spinal dorsal horns of the rat. J Comp Neurol 457:236–249.

Light AR, Perl ER (1979) Spinal termination of functionally identified primary afferent neurons with slowly conducting myelinated fibers. J Comp Neurol 186:133–150.

Light AR, Perl ER (2003) Unmyelinated afferent fibers are not only for pain anymore. J Comp Neurol 461:137–139.

Lochter A, Galosy S, Muschler J, Freedman N, Werb Z, Bissell MJ (1997) Matrix metalloproteinase stromelysin-1 triggers a cascade of molecular alterations that leads to stable epithelial-to-mesenchymal conversion and a premalignant phenotype in mammary epithelial cells. J Cell Biol 139:1861–1872.

Mandai K, Nakanishi H, Satoh A, Obaishi H, Wada M, Nishioka H, Itoh M, Mizoguchi A, Aoki T, Fujimoto T, Matsuda Y, Tsukita S, Takai Y (1997) Afadin: a novel actin filament-binding protein with one PDZ domain localized at cadherin-based cell-to-cell adherens junction. J Cell Biol 139:517–528.

Mantyh PW, Rogers SD, Honore P, Allen BJ, Ghilardi JR, Li J, Daughters RS, Lappi DA, Wiley RG, Simone DA (1997) Inhibition of hyperalgesia by ablation of lamina I spinal neurons expressing the substance P receptor. Science 278:275–279.

Marambaud P, Shioi J, Serban G, Georgakopoulos A, Sarner S, Nagy V, Baki L, Wen P, Efthimiopoulos S, Shao Z, Wisniewski T, Robakis NK (2002) A presenilin-1/gamma-secretase cleavage releases the E-cadherin intracellular domain and regulates disassembly of adherens junctions. EMBO J 21:1948–1956.

Marthiens V, Padilla F, Lambert M, Mege RM (2002) Complementary expression and regulation of cadherins 6 and 11 during specific steps of motoneuron differentiation. Mol Cell Neurosci 20:458–475.

Molander C, Wang HF, Rivero-Melian C, Grant G (1996) Early decline and late restoration of spinal cord binding and transganglionic transport of isolectin B4 from Griffonia simplicifolia I after peripheral nerve transection and crush. Restor Neurol Neuros 10:123–133.

Murase S, Mosser E, Schuman EM (2002) Depolarization drives beta-catenin into neuronal spines promoting changes in synaptic structure and function. Neuron 35:91–105.

Nagafuchi A, Takeichi M (1988) Cell binding function of E-cadherin is regulated by the cytoplasmic domain. EMBO J 7:3679–3684.

Nishioka H, Mizoguchi A, Nakanishi H, Mandai K, Takahashi K, Kimura K, Satoh-Moriya A, Takai Y (2000) Localization of l-afadin at puncta adhaerentia-like junctions between the mossy fiber terminals and the dendritic trunks of pyramidal cells in the adult mouse hippocampus. J Comp Neurol 424:297–306.

Peters A, Palay SL, Webster HD (1991) The fine structure of the nervous system. New York: Oxford UP.

Poskanzer K, Needleman LA, Bozdagi O, Huntley GW (2003) N-cadherin regulates ingrowth and laminar targeting of thalamocortical axons. J Neurosci 23:2294–2305.

Price SR, De Marco Garcia NV, Ranscht B, Jessell TM (2002) Regulation of motor neuron pool sorting by differential expression of type II cadherins. Cell 109:205–216.

Ribak CE, Vaughn JE, Saito K (1978) Immunocytochemical localization of glutamic acid decarboxylase in neuronal somata following colchicine inhibition of axonal transport. Brain Res 140:315–332.

Ribeiro-da-Silva A, Coimbra A (1982) Two types of synaptic glomeruli and their distribution in laminae I-III of the rat spinal cord. J Comp Neurol 209:176–186.

Roura S, Miravet S, Piedra J, Garcia de Herreros A, Dunach M (1999) Regulation of E-cadherin/catenin association by tyrosine phosphorylation. J Biol Chem 274:36734–36740.

Ruda MA, Bennett GJ, Dubner R (1986) Neurochemistry and neural circuitry in the dorsal horn. Prog Brain Res 66:219–268.

Schaible HG (1996) On the role of tachykinins and calcitonin gene-related peptide in the spinal mechanisms of nociception and in the induction and maintenance of inflammation-evoked hyperexcitability in spinal cord neurons (with special reference to nociception in joints). Prog Brain Res 113:423–441.

Seto A, Hasegawa M, Uchiyama N, Yamashima T, Yamashita J (1997) Alteration of E-cadherin and alpha N-catenin immunoreactivity in the mouse spinal cord following peripheral axotomy. J Neuropathol Exp Neurol 56:1182–1190.

Shan W, Yoshida M, Wu XR, Huntley GW, Colman DR (2002) Neural (N-) cadherin, a synaptic adhesion molecule, is induced in hippocampal mossy fiber axonal sprouts by seizure. J Neurosci Res 69:292–304.

Shehab SA, Spike RC, Todd AJ (2003) Evidence against cholera toxin B subunit as a reliable tracer for sprouting of primary afferents following peripheral nerve injury. Brain Res 964:218–227.

Shimamura K, Takahashi T, Takeichi M (1992) E-cadherin expression in a particular subset of sensory neurons. Dev Biol 152:242–254.

Shortland P, Woolf CJ, Fitzgerald M (1989) Morphology and somatotopic organization of the central terminals of hindlimb hair follicle afferents in the rat lumbar spinal cord. J Comp Neurol 289:416–433.

Steinhusen U, Weiske J, Badock V, Tauber R, Bommert K, Huber O (2001) Cleavage and shedding of E-cadherin after induction of apoptosis. J Biol Chem 276:4972–4980.

Sugimoto T, Gobel S (1982) Primary neurons maintain their central axonal arbors in the spinal dorsal horn following peripheral nerve injury: an anatomical analysis using transganglionic transport of horseradish peroxidase. Brain Res 248:377–381.

Sugiura Y, Lee CL, Perl ER (1986) Central projections of identified, unmyelinated (C) afferent fibers innervating mammalian skin. Science 234:358–361.

Sun RQ, Lawand NB, Willis WD (2003) The role of calcitonin gene-related peptide (CGRP) in the generation and maintenance of mechanical allodynia and hyperalgesia in rats after intradermal injection of capsaicin. Pain 104:201–208.

Szentágothai J (1964) Neuronal and synaptic arrangement in the substantia gelatinosa Rolandi. J Comp Neurol 122:219–239.

Tanaka H, Shan W, Phillips GR, Arndt K, Bozdagi O, Shapiro L, Huntley GW, Benson DL, Colman DR (2000) Molecular modification of N-cadherin in response to synaptic activity. Neuron 25:93–107.

Tandrup T, Woolf CJ, Coggeshall RE (2000) Delayed loss of small dorsal root ganglion cells after transection of the rat sciatic nerve. J Comp Neurol 422:172–180.

Tang L, Hung CP, Schuman EM (1998) A role for the cadherin family of cell adhesion molecules in hippocampal long-term potentiation. Neuron 20:1165–1175.

Todd AJ, Spike RC (1993) The localization of classical transmitters and neuropeptides within neurons in laminae I-III of the mammalian spinal dorsal horn. Prog Neurobiol 41:609–645.

Todd AJ, Hughes DI, Polgar E, Nagy GG, Mackie M, Ottersen OP, Maxwell DJ (2003) The expression of vesicular glutamate transporters VGLUT1 and VGLUT2 in neurochemically defined axonal populations in the rat spinal cord with emphasis on the dorsal horn. Eur J Neurosci 17:13–27.

Tong YG, Wang HF, Ju G, Grant G, Hokfelt T, Zhang X (1999) Increased uptake and transport of cholera toxin B-subunit in dorsal root ganglion neurons after peripheral axotomy: possible implications for sensory sprouting. J Comp Neurol 404:143–158.

Uchida N, Honjo Y, Johnson KR, Wheelock MJ, Takeichi M (1996) The catenin/cadherin adhesion system is localized in synaptic junctions bordering transmitter release zones. J Cell Biol 135:767–779.

Uchiyama N, Hasegawa M, Yamashima T, Yamashita J, Shimamura K, Takeichi M (1994) Immunoelectron microscopic localization of E-cadherin in dorsal root ganglia, dorsal root and dorsal horn of postnatal mice. J Neurocytol 23:460–468.

van Lookeren Campagne M, Oestreicher AB, van der Krift TP, Gispen WH, Verkleij AJ (1991) Freeze-substitution and Lowicryl HM20 embedding of fixed rat brain: suitability for immungold ultrastructural localization of neural antigens. J Histochem Cytochem 39:1267–1279.

Vulchanova L, Olson TH, Stone LS, Riedl MS, Elde R, Honda CN (2001) Cytotoxic targeting of isolectin IB4-binding sensory neurons. Neuroscience 108:143–155.

Wang X, Weiner JA, Levi S, Craig AM, Bradley A, Sanes JR (2002) Gamma protocadherins are required for survival of spinal interneurons. Neuron 36:843–854.

Weinberg RJ, van Eyck SL (1991) A tetramethylbenzidine/tungstate reaction for horseradish peroxidase histochemistry. J Histochem Cytochem 39:1143–1148.

Woolf CJ, Salter MW (2000) Neuronal plasticity: increasing the gain in pain. Science 288:1765–1769.

Woolf CJ, Shortland P, Coggeshall RE (1992) Peripheral nerve injury triggers central sprouting of myelinated afferents. Nature 355:75–78.

Woolf CJ, Shortland P, Reynolds M, Ridings J, Doubell T, Coggeshall RE (1995) Reorganization of central terminals of myelinated primary afferents in the rat dorsal horn following peripheral axotomy. J Comp Neurol 360:121–134.

Xie Y, Zhang J, Petersen M, LaMotte RH (1995) Functional changes in dorsal root ganglion cells after chronic nerve constriction in the rat. J Neurophysiol 73:1811–1820.

Yamagata M, Herman JP, Sanes JR (1995) Lamina-specific expression of adhesion molecules in developing chick optic tectum. J Neurosci 15:4556–4571.

Yap AS, Brieher WM, Gumbiner BM (1997) Molecular and functional analysis of cadherin-based adherens junctions. Annu Rev Cell Dev Biol 13:119–146.

Zhang B, Levitt P, Murray M (1998) Induction of presynaptic reexpression of an adhesion protein in lamina II after dorsal root deafferentation in adult rat spinal cord. Exp Neurol 149:468–472.